Available online at www.CivileJournal.org

Civil Engineering Journal

(E-ISSN: 2476-3055; ISSN: 2676-6957)

Vol. 12, No. 05, May, 2026

Monitoring Compressive Strength Development of Mortar Using Cement-Based Piezoelectric Composite Under Low Electric Field Polarization

Gati Annisa Hayu [1, 2], Wahyuniarsih Sutrisno [1], Kiki Dwi Wulandari [1, 3], Priyo Suprobo [1*]

[1] *Department of Civil Engineering, Sepuluh Nopember Institute of Technology, Surabaya, East Java 60111, Indonesia.*

[2] *Department of Civil Engineering, Universitas Pertamina, Jakarta Selatan, DKI Jakarta 12220, Indonesia.*

[3] *Politeknik Perkapalan Negeri Surabaya, Surabaya, Indonesia.*

Received 16 June 2025; Revised 29 March 2026; Accepted 07 April 2026; Published 01 May 2026

Abstract

The Cement-based Piezoelectric Composite (CPC) used in this research is a 0-3 type, composed of Lead Zirconate Titanate (PZT) powder and cement with a 50:50 volume ratio. The CPC was produced under low electric field polarization with specific durations: C1 (250 V/mm, 40 minutes), C2 (250 V/mm, 60 minutes), C3 (375 V/mm, 40 minutes), and C4 (375 V/mm, 60 minutes). CPC was embedded inside the mortar to monitor the strength development for 90 days using the Electromechanical Impedance (EMI) technique. The results show that the conductance decreases (resistance increases) as the compressive strength increases. A more thorough analysis was conducted using the Root Mean Square Deviation (RMSD) technique, which serves as an effective indicator of concrete strength development and damage. This analysis aims to establish a quantitative correlation between the sensor's conductance and the mortar's strength as it develops. The results show that the increase in compressive strength corresponds with an increase in conductance RMSD, which indicates the sensor sensitivity. Furthermore, the C4 sample exhibits the greatest sensitivity and capability for monitoring the development of compressive strength. Even though the d_{33} values are relatively low, at 4.87 pC/N, C4 can detect the compressive strength up to 90 days with a broad frequency range of 300-1000 kHz. CPC with low electric field polarization can still be utilized as an embedded sensor to monitor the development of compressive strength in cementitious materials.

Keywords: Cement-Based Piezoelectric Composite; Compressive Strength Monitoring; Lead Zirconate Titanate; Low Electric Field Polarization; Structural Health Monitoring.

1. Introduction

Considering the deterioration of concrete structures due to internal and external factors, the structural health monitoring system (SHM) must anticipate the damage to the structure. The presence of SHM can prevent structural damage, extend service life, and reduce maintenance costs by detecting damage and reductions in structural strength early on. Among several techniques in SHM, Piezoelectric is the most effective mechanism. It has been widely used as a sensor due to its unique electromechanical properties, allowing it to be utilized as both a sensor and an actuator [1]. The use of piezoelectric materials, such as piezoelectric ceramics and polymers, as embedded sensors in concrete has garnered attention and continues to be developed. While these conventional materials may be appropriate for steel reinforcement, masonry, or steel structures, they are not ideal for concrete structures [2–6]. Concrete undergoes

* Corresponding author: priyo@its.ac.id

https://doi.org/10.28991/CEJ-2026-012-05-08

shrinkage and expansion during the hydration process due to internal and external factors. In such cases, the intelligent material sensor does not shrink in sync with the concrete, leading to partial energy loss in the signal. Furthermore, the density difference between piezoelectric materials (4.64-7.6×10³ kg/m³) and concrete (2.4×10³ kg/m³) creates a substantial acoustic impedance mismatch. Since acoustic impedance is crucial for sensor data acquisition, this large discrepancy causes signal reception issues [7]. As a result, conventional piezoelectric materials are considered unsuitable for use in concrete structures.

To overcome the impedance mismatch problem between piezoelectric sensors and concrete as host materials, many researchers have developed sensors consisting of cement and piezoelectric materials [8–11]. This composite material is known as Cement-based Piezoelectric Composite (CPC). Since its initial development, several connectivity configurations have been proposed for cement-based piezoelectric composites. Among them, the 0-3 type has become the most widely adopted. The term "0-3" describes the dimensional relationship between the two phases: the piezoelectric ceramic particles are dispersed as a 0-dimensional phase within a continuous 3-dimensional cement matrix. This type of composite is typically fabricated by uniformly mixing piezoelectric powder with cement. In other words, piezoelectricity is dispersed in all directions [7, 12–15]. Several studies have investigated the performance and potential of 0–3 cement–piezoelectric composites. Li et al. [16] demonstrated that 0–3 cement–PZT composites can be effectively applied in civil engineering and exhibit better compatibility with concrete than pure PZT sensors. Wang et al. [17] highlighted that 0–3 cement–PZT composites show enhanced frequency response and piezoelectric performance, confirming that the 0–3 configuration remains a relevant and practical option.

Potong et al. [18] and Chomyen et al. [19] further examined how 0–3 connectivity affects the electrical properties and microstructure of the composite. In a comprehensive review, Ding et al. [7] and Yang et al. [20] reaffirmed that the 0–3 configuration remains widely used, despite some limitations compared to 1–3 and 2–2 connectivities. A study conducted by Ma et al. [21] showed an increase in sensitivity at 1-3 connectivity. However, this connectivity requires high geometry and orientation control, compared to 0-3, which is more practical and durable for structural-scale applications. Based on these previous studies, several factors contribute to the continued popularity of the 0–3 type configuration: 1) simple fabrication process, in which the piezoelectric materials are randomly dispersed in a cement matrix; 2) good mechanical compatibility, in which cement matrix provides mechanical strength while piezoelectric material contributes to the sensing ability; 3) a homogenous distribution benefits applications requiring consistent sensor performance across a large area; and 4) cost-effectiveness. This type offers a practical balance between functionality and manufacturability.

In a CPC, the polarization process is the most crucial and challenging phase. This process involves applying a constant external electric field to the piezoelectric material, thereby reorienting its spontaneous polarization [8–10, 22]. The effectiveness of the poling process is paramount as it directly influences the piezoelectric properties of the material. Factors such as the electric field strength, temperature, and the duration of application play a crucial role in determining the success of the polarization process [6, 23, 24]. Pan et al. [25–27] applied an electric field of 1.5 kV/mm at a constant temperature of 150°C for a period of 40 minutes and obtained a d_{33} value greater than 90 pC/N. The CPC sensor performed stably in the frequency range exceeding 800 kHz. Santos et al. [1] demonstrated that the application of an electric field of 2 kV/mm at a temperature of 90°C produces effective dipole orientation, even though it might lead to dielectric breakdown in mortar. Chomyen et al. [19] supported this notion by using an electric field of 0.5 kV/mm at a temperature of 60°C, concluding that the contribution of heat energy is a must for the process of effective polarization. Overall, these findings suggest that all past studies continue to rely on the combination of high-temperature and high-field conditions to achieve high d_{33} and high sensor sensitivity. Although higher electric fields (1-4 kV/mm) are commonly used in the polarization process and are well-documented [3, 11, 25, 28, 29], low electric fields also present promising potential. In piezoelectric specimens, low electric fields can prevent dielectric breakdown and prevent the occurrence of unwanted electrochemical reactions that negatively impact the composite's properties. Additionally, low electric fields yield more controlled and homogeneous polarization throughout the material, resulting in more consistent and reliable results. Li et al. [23] experimented on the 0-3 type cement-based Lead Zirconate Titanate (PZT) under several external electric fields, including an electric field of 330 V/mm, which was categorized as a low electric field. The results showed that the piezoelectric strains (d_{33}) remained approximately 5 pC/N for 180 days.

The combination of PZT sensors with Electromechanical Impedance (EMI) technology has proven to be a highly effective and beneficial practice for monitoring civil structures. The study has demonstrated that variations in the impedance/conductance spectrum of the PZT sensor mirror closely correlate with changes in the strength and stiffness of the host material, thereby indicating age, hydration, and even mechanical damage. Li et al. [30] used a PZT-EMI technique as a monitoring system for detecting and localizing damage in concrete structures. Their results showed that variations in impedance signatures are sensitive to the changes in local stiffness and can effectively reflect the mechanical condition of the host concrete. In the same vein, Pan et al. [25] employed the PZT-EMI sensor technique for monitoring the growth of mortar compressive strength, and it was found that the RMSD of conductance and spectrum

shift were closely linked to the rise in strength. Additionally, Jothi Saravanan et al. [31] demonstrated the ability of PZT to monitor the early strength gain and the presence of cracks in test elements by showing that the EMI signature changed remarkably as the cracks developed. Wang et al. [17] illustrated the use of EMI-PZT for monitoring cracks in structures, thereby affirming the application of EMI for identifying localized damage. Pan et al. [32] report the detection of the stress-strain relationship during the stepwise compression testing by PZT sensors. However, the outcome was not as favorable as the EMI signature from CPC sensors.

Gedam et al. [33] measured the beam conductance and susceptance using embedded smart aggregate-based sensors to detect damage in concrete. The results show that using the EMI technique, the early damage level of the concrete beam could be easily detected, and the level of PZT sensitivity depends on the location of the sensors relative to the damage location. The nearer the sensor position to the damage location, the higher the sensitivity recorded. Saravanan et al. [31] utilized PZT sensors to monitor early-stage characteristics (1-3 days) and later-stage strength gain (3-28 days) by studying the EMI signatures. Wang et al. [34] used bonded PZT sensors to detect small cracks in plate-like structures by measuring the change in the EMI. Experimental results revealed that the peak admittance frequency decreased as the crack size increased. The Piezoelectric sensor-based EMI technique is one of the most effective methods in structural health monitoring, and it has been continually developed due to its ease of signal interpretation and high-frequency detection [27, 35, 36]. The literature indicates that PZT-based EMI methods have developed into non-destructive monitoring tools for the following main applications: 1) tracking the development of strength and modulus at the early age, 2) crack and damage monitoring, 3) registering stress-strain in concrete structures. The constant demand for sensors that can work effectively with concrete mixtures has led to the use of CPC in conjunction with EMI methods, which were initially proven reliable with PZT sensors.

Generally, the EMI technique has proven to be very useful in monitoring the strength development of cement-based structures. Meanwhile, the CPC sensor-based EMI technique still needs to be expanded to concrete structures. Pan et al. [27] monitored the strength development of concrete cylinders and the damage to concrete beams. The results show that CPC's sensitivity (based on impedance and conductance values) is better than conventional PZT and is applicable as SHM in concrete structures. Pan & Huang [25] monitored the development of concrete strength over a period of 56 days. The study reported that the acoustic impedance of the composite was closer to the impedance of the concrete structure. Pan and Guan [32] investigated the stress-strain relationship of concrete using the EMI technique. The results show that the frequency range of the CPC is broader than that of the conventional PZT. The analysis of the CPC conductance spectrum is more accessible and takes a shorter time than conventional PZT. CPC could be used to monitor stress and strain during loading.

Previous studies indicate that the low electric fields are currently limited to a maximum of 330 V/mm, while electric fields of 250 V/mm and 375 V/mm present additional opportunities for exploration. Results from earlier polarization trials, which tested durations of 40, 60, 90, and 120 minutes, revealed that 40 and 60 minutes produced the highest d_{33} values. In contrast, the longer duration of 90 and 120 minutes did not significantly affect the d_{33} values, and some samples were damaged during these extended tests. This study aims to evaluate the performance of CPC sensors polarized under low electric fields in monitoring the strength development of mortar using the CPC-based Electromechanical Impedance (CPC-EMI) technique. Four variations were prepared: C1 (250 V/mm, 40 minutes), C2 (250 V/mm, 60 minutes), C3 (375 V/mm, 40 minutes), and C4 (375 V/mm, 60 minutes). The CPC sensors were embedded at the center of the mortar specimen for 90 days, and both conductance spectra and compressive strength were measured at 7, 28, 56, and 90 days. The sensing capability of each sensor was analyzed by comparing the conductance-compressive strength Root Mean Square Deviation (RMSD) relationships among all variants. Conventional PZT sensors were also used and embedded inside mortar for comparison. The remainder of this paper is organized as follows: Section 2 describes the fabrication process, properties, and packaging of the CPC sensors, and explanation about EMI technique; Section 3 presents and discusses the relationship between conductance and age, conductance and compressive strength, conductance RMSD and compressive strength, and the potential use of the CPC; Section 4 concludes the key findings and implication of this study.

2. Experimental Procedure

2.1. Fabrication Process of Piezoelectric Composite

PZT is the most used piezoelectric material for sensors in SHM due to its favorable electrical properties and ease of polarization [3, 6, 23, 37, 38]. In this study, PZT crystalline powder, with an average particle size of 100-120 nm and a purity of 99.9%, was employed as the functional phase in the mixture. The PZT powder consists of 52 mol% Lead Zirconate ($PbZrO_3$) and 48 mol% Lead Titanate ($PbTiO_3$), with a density of 7.7 g/cm³. Ordinary Portland Cement (OPC), with a density of 3.03 g/cm³, was used as the matrix phase. The OPC primarily consists of CaO, SiO_2, Fe_2O_3, and Al_2O_3 in proportions of 76.6%, 9.83%, 5.68%, and 1.70%, respectively. Figure 1 the granulation diagram of the PZT.

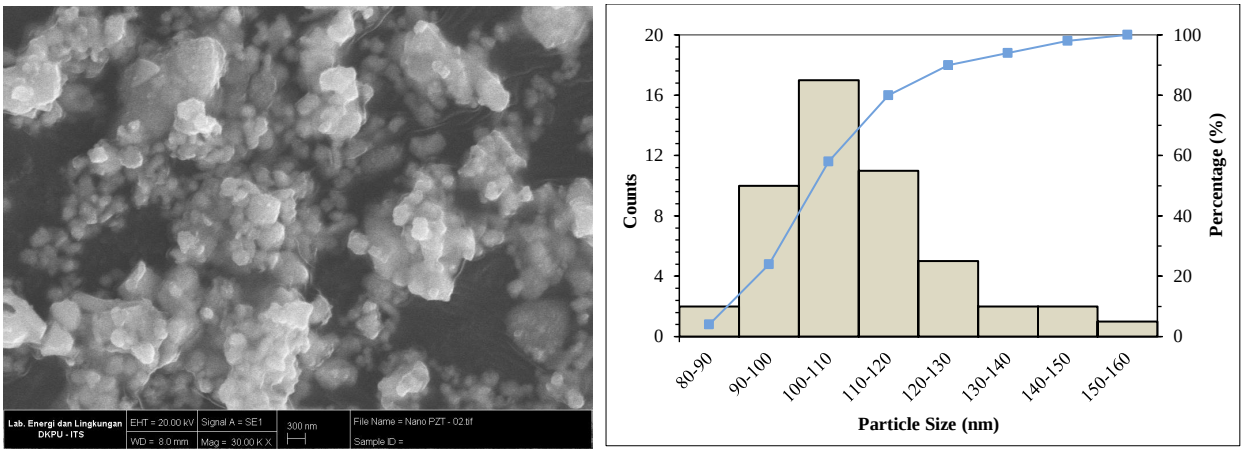

Figure 1. Granulation profiles of the PZT powder

The 0-3 CPCs, a key component of this study, were produced by uniformly mixing the PZT powder and cement in a 50:50 volume ratio. The mixture was then placed in a steel mold with a diameter of 20 mm and a thickness of 2 mm. The steel mold was then compressed by applying 80 MPa to compact the sensor specimen. The specimens were cured at 90°C and 100% relative humidity for 24 hours. Prior to polarization, the specimens were placed into an oven at 140°C for 40 minutes. This process was conducted to improve the polarization efficiency of the specimen because it can reduce moisture [7, 29]. After pre-treatment, the specimens were polished and coated with low-temperature silver paint to create electrodes on both surfaces. Post-treatment with the same condition as pre-treatment was then conducted before the polarization. Figure 2 shows CPC specimens that have been polished and coated with silver paint.

Figure 2. CPC sensor specimens prepared with four polarization variations

The polarization process was conducted by immersing the specimen in a silicone oil bath heated to a specific temperature. An electric field was then applied for a designated period. Chaipanich [29] polarized the piezoelectric composite at an electric field of 2 kV/mm for 45 minutes. Similarly, Jaitanong & Chaipanich [28] selected a field strength of 1 kV/mm and a duration of 45 minutes for the polarization of the piezoelectric composite. In contrast, Pan and Huang [25] performed polarization at 1.5 kV/mm for 40 minutes, while Shifeng et al. [39] used an electric field of 4 kV/mm for 45 minutes. Qin et al. [3] also conducted polarization at 4 kV/mm. These previous studies indicate that the polarization conditions typically involve high electric field strengths. On the other hand, Dong & Li [40] investigated the effects of various electric fields, including 330 V/mm, 27 kV/cm, and 43 kV/cm, with the low electric field limited to 330 V/mm. In the early experiments of the current study, four different polarization durations were tested: 40, 60, 90, and 120 minutes. Results showed that the durations of 90 and 120 minutes did not significantly affect the d_{33} value when compared to 40 and 60 minutes; in fact, some samples were damaged during the process. In this study, low external electric fields of 250 V/mm and 375 V/mm were applied. The choice of low external electric fields is significant because it allows for a controlled and gradual polarization process, which is crucial for the quality and reliability of the results. With a specimen thickness of 2 mm, the corresponding voltages were 500 V and 750 V, which fall into the low-voltage range. The polarization durations used were 40 and 60 minutes. The specimens were stored in Styrofoam to preserve their polarized state. A disk-like PZT ceramic patch with a diameter of 20 mm and a thickness of 2 mm was prepared for comparison with the CPC specimen.

CPC consists of PZT particles randomly dispersed within the cement matrix, forming 0–3 connectivity. This even particle dispersion provides advantages when CPC is used as an embedded sensor in mortar. One of its main advantages is high mechanical compatibility, as the elastic modulus of CPC is close to that of cement, allowing stress to be transferred more effectively. In addition, the EMI interaction generated by CPC is more stable because there is no extreme difference in stiffness, as in pure PZT sensors that are attached or embedded in mortar. In composites with

connectivity of 0–3, the cement pastes acts as a three-dimensional (3D) continuous phase, meaning that the cement matrix is interconnected throughout the composite volume without interruption. PZT particles are only a 0-dimensional dispersed phase embedded in the matrix. This configuration causes the mechanical properties of CPC to be determined more by the cement matrix, while PZT contributes to the piezoelectric response. Thus, the effective modulus of CPC lies between those of the two materials but is closer to that of cement. This condition results in improved mechanical compatibility and reduces stiffness mismatch at the interface, thereby stabilizing the EMI response of the embedded CPC sensor. In terms of durability, CPC tends to be more durable and does not experience delamination, a common issue found in PZT patches. The disadvantage is that the $d_{3\ 3}$ value is relatively lower than pure PZT. However, in EMI technology, this is not a major obstacle because EMI sensitivity does not only depend on high piezoelectric output, but also on the stability of the impedance/conductance signal recorded due to mechanical interaction with the surrounding material.

2.2. Properties of Piezoelectric Composite Specimen

The properties of CPC specimens, including piezoelectric strain coefficient (d_{33}), capacitance (C), dielectric constant (ε_r), and piezoelectric voltage coefficient (g_{33}), were measured with utmost precision and care over a 30-day period in the temperature-controlled room. The values of these properties, which represent the average of six specimens, were obtained through a rigorous experimental process. For comparison, a commercially ordered disk-shaped PZT ceramic patch was also prepared, with a diameter of 20 mm and a thickness of 2.08 mm. This PZT patch was ready for testing, conducted 30 days after the polarization process, to ensure that it was in the same condition as the other CPCs during piezoelectric properties tests. The d_{33} values for both the PZT and CPC materials were measured using the YE2730A-type piezometer. The results, illustrated in Figure 3, highlight the meticulousness of our approach.

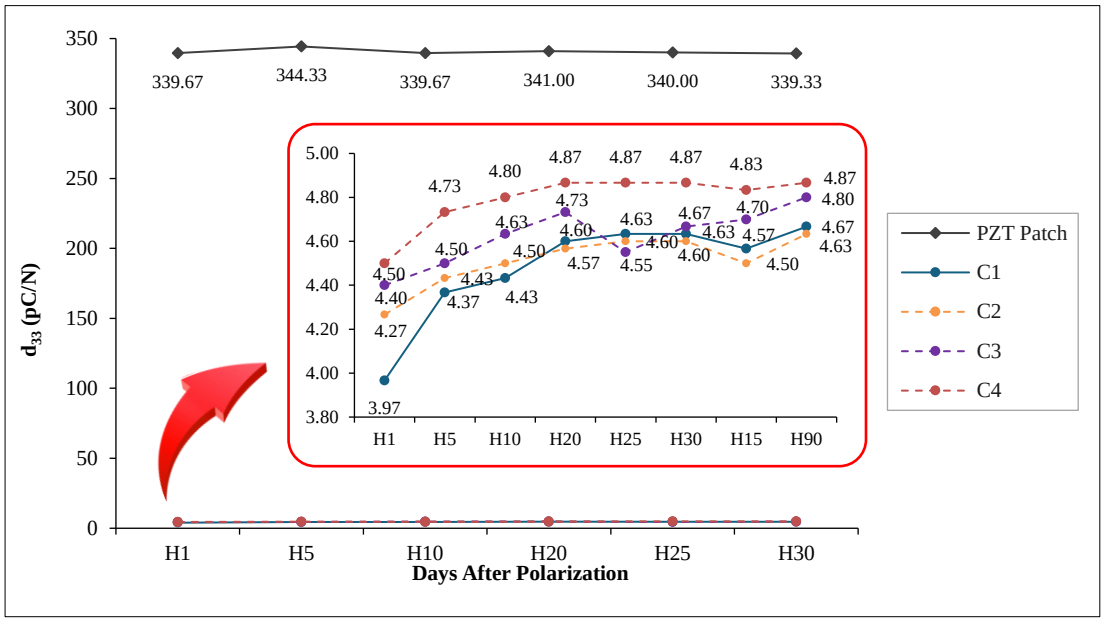

Figure 3. Measured d_{33} values of the CPC for each polarization condition

The d_{33} value of PZT sensors showed no significant variation with aging over a 30-day period. Meanwhile, the d_{33} value of CPC was sensitive to age. As the specimen age increased, the d_{33} values increased and tended to become stable at days 25 and 30. This sensitivity can be attributed to the hydration process experienced by the cements in CPC. The primary product of this process is C-S-H, which plays a crucial role in binding the composite together. C-S-H can improve the density of the composite and can reduce the composite's damage [41]. The local stress inside the specimens increased, which is related to continuous hydration and moisture absorption [10, 42]. These results align with previous studies. Li et al. [16] investigated the effects of polarizing voltage and duration on cement-based PZT composites. Their study concluded that both the voltage and duration significantly enhanced the d_{33} values. Additionally, they found that the d_{33} values tended to increase as the composites aged [40]. In a separate study, Pan and Huang [25] examined the relationship between the age of a specimen and the d_{33} values of piezoelectric cement sensors. They discovered that the specimen's age influenced these values. In contrast, conventional PZT exhibited significantly higher d_{33} values than piezoelectric cement sensors, and these values remained insensitive to aging [25]. Wang et al. [17] found that the d_{33} values of cement-based piezoelectric composites increased rapidly during the first 38 days after poling, followed by a slower increase over the next 50 days, and remained relatively constant after 90 days [17]. The studies indicate that these phenomena are related to the hydration process of the cement. Among the polling condition variations, C4 showed the most significant value of d_{33}. The d_{33} values of all variants are relatively low. This condition is due to the low external

electric field applied during the polarization process. The external electric field is a driving force that aligns the direction of the dipoles inside the CPC. The low electric field resulted in a low driving force, so the alignment of the dipole direction is not optimal, leading to low d_{33} [28].

The C values were obtained using an Inductance, Capacitance, and Resistance (LCR) meter at a 1 kHz frequency. This value was used to calculate the ε_r. The C and ε_r are relatable but describe different systems and electrical materials concepts. The C4 showed the biggest capacitance, followed by C2, C3, and C1, with values of 78.97 pF, 75.59 pF, 73.02 pF, and 66.29 pF, respectively. Regarding dielectric constant, C4 showed the most significant value, followed by C2, C3, and C1, with values of 85.32, 73.99, 73.54, and 64.16, respectively. This result showed that C4 was the sample with the best capability to conserve electrical energy when subjected to an electric field compared to the other samples. Figure 4 shows a comparison of the capacitance and dielectric constant of the four CPC variations. The highest piezoelectric voltage coefficient (g_{33}) values are found in C1 and C3, with measurements of 8.6×10^{-3} Vm/N and 7.5×10^{-3} Vm/N, respectively. The g_{33} value is the opposite of the ε_r value.

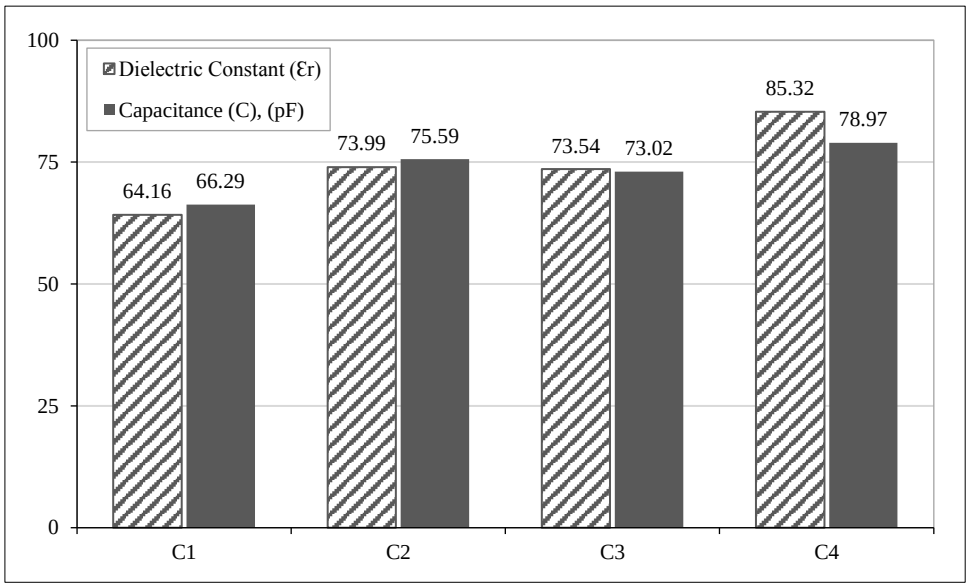

Figure 4. Dielectric constant and capacitance of CPC obtained from LCR meter measurement

2.3. Packaging of CPC and Cement Mortar

After verifying the piezoelectric properties, the CPC sensors were prepared for embedding in cement mortar. The copper foil, serving as the conductive wires, was meticulously attached to the electrode surfaces of the CPC sensor. The cement paste covered all the parts of the CPC sensor and half the length of the copper foil, highlighting the crucial role of the sensor in the investigation. The copper foil was then wrapped in the heat-shrinkable thermal casing, ensuring the sensor's protection and functionality, as depicted in Figure 5. The mortar mixture consisted of 500 g of OPC, 1375 g of sand, and 225 mL of water. This mixture was then cast into a steel mold of 5 x 5 x 5 cm^3. To investigate the strength development of the mortar, the CPC sensor was placed at the center of the mortar cube.

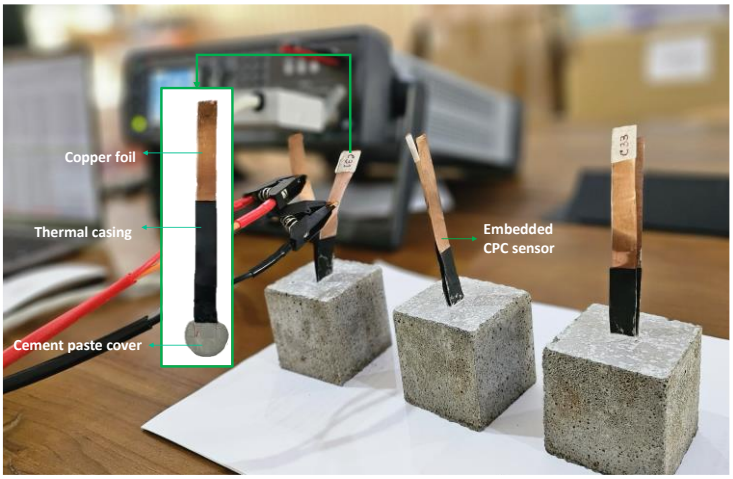

Figure 5. Embedded CPC sensor positioned at the canter of the mortar specimen

2.4. EMI Technique and Compressive Strength Testing

The initial hydration of cementitious materials results in significant changes to their mechanical properties, including increased stiffness, enhanced load-bearing capacity, and reduced porosity. The microstructural changes have a direct impact on the mechanical impedance of the material; hence, the changes in the conductance spectrum are quite similar. The embedded piezoelectric sensor, which is a crucial technology in our research, records this spectrum. The effective frequency range, where conductance regularly depends on age, is the best zone for monitoring the changes in mechanical properties. Within this range, conductance tends to increase as frequency increases and decrease as the mortar becomes stiffer. Consequently, the EMI signature offers a non-destructive, high-resolution means of gaining insight into the time-dependent mechanical behavior of cementitious materials.

Due to its adaptability and cost-effectiveness, the EMI technique is widely used in SHM and Non-destructive Tests (NDT) for various engineering problems. The structure under examination is equipped with a PZT sensor, either surface-bonded or embedded, and stimulated by an alternating voltage signal using an impedance analyzer or LCR meter [25, 31]. This technique has been successfully applied to detect the development of concrete's compressive strength and damage, thanks to its ease of signal interpretation. The EMI technique is based on the dynamic equation of the dynamic sensors and the stiffness of the structure. The electrical admittance ($\bar{Y}$), which is the inverse of the impedance of the piezoelectric material, is governed by Equation 1. This equation suggests that a change in the mechanical properties of the host structure will result in a corresponding change in mechanical impedance, potentially leading to a variation in electrical impedance [33].

$$\bar{Y} = G + iB = 4\omega i \frac{l^2}{h}\left[\overline{\varepsilon_{33}^{T}} - \frac{2d_{31}^2\overline{Y^E}}{(1-\nu)} + \frac{2d_{31}^2\overline{Y^E}}{(1-\nu)}\left(\frac{Z_{a,eff}}{Z_{s,eff}+Z_{a,eff}}\right)\bar{T}\right] \quad (1)$$

where G, B, i, l, and h represent conductance, susceptance, imaginary unit, half-length, and the thickness of the piezoelectric material, respectively. ε_{33}^{T} is complex electric permittivity, Y^E is the complex Young's modulus of piezoelectric material, v is Poisson's ratio of piezoelectric material, T is the complex tangent ratio, $Z_{a,eff}$ is the mechanical impedance of piezoelectric material, and $Z_{s,eff}$ is the mechanical impedance of the structure. In SHM and NDT with EMI techniques, impedance (Z) and conductance (G) are used to characterize the dynamic behavior of a structure. These two parameters can be analyzed to extract meaningful information regarding the structure's health. If Z is identical to the overall electrical-mechanical interaction, G is more suitable or sensitive to detect specific structural changes or damage.

This study recorded the EMI response of the embedded CPC sensors in the form of conductance signals using an LCR meter with a frequency range of 20 kHz to 1000 kHz. The conductance of each specimen was measured periodically on days 7, 28, 56, and 90 to capture the electromechanical signatures reflecting the strength development of the mortar. Each conductance value was then compared with the baseline conductance obtained 6 hours after casting. This quantification process is referred to as the Root Mean Square Deviation (RMSD), which represents the statistical difference between the conductance at a specific age (days 7, 28, 56, and 90) and the baseline value. The calculation was performed within the effective frequency range. This range, determined through a series of preliminary tests, exhibits consistent conductance trends over mortar age and is crucial for ensuring the accuracy of the results. RMSD serves as a statistical indicator to evaluate the deviation of conductance over time or between specimens in cement-based piezoelectric composite measurements [43]. The conductance RMSD (G_R) was calculated according to Equation 2 as follows:

$$G_R = \sqrt{\frac{\sum_{i=1}^{n}(G_i - G_i^0)^2}{\sum_{i=1}^{n}(G_i^0)^2}} \quad (2)$$

where G_i and G_i^0 represent conductance at frequency i and baseline conductance at frequency i, respectively. n is the number of frequency points considered in the effective frequency range. Additionally, compressive strength tests were conducted on the same specimens at the same ages to validate the EMI results destructively. Although the compressive test caused total failure of the specimens, the correlation between the conductance RMSD and the measured compressive strength suggests that the material's performance developed progressively rather than being damaged by external loading. Figure 6 illustrates the schematic diagram of this study, which describes the methodology's process.

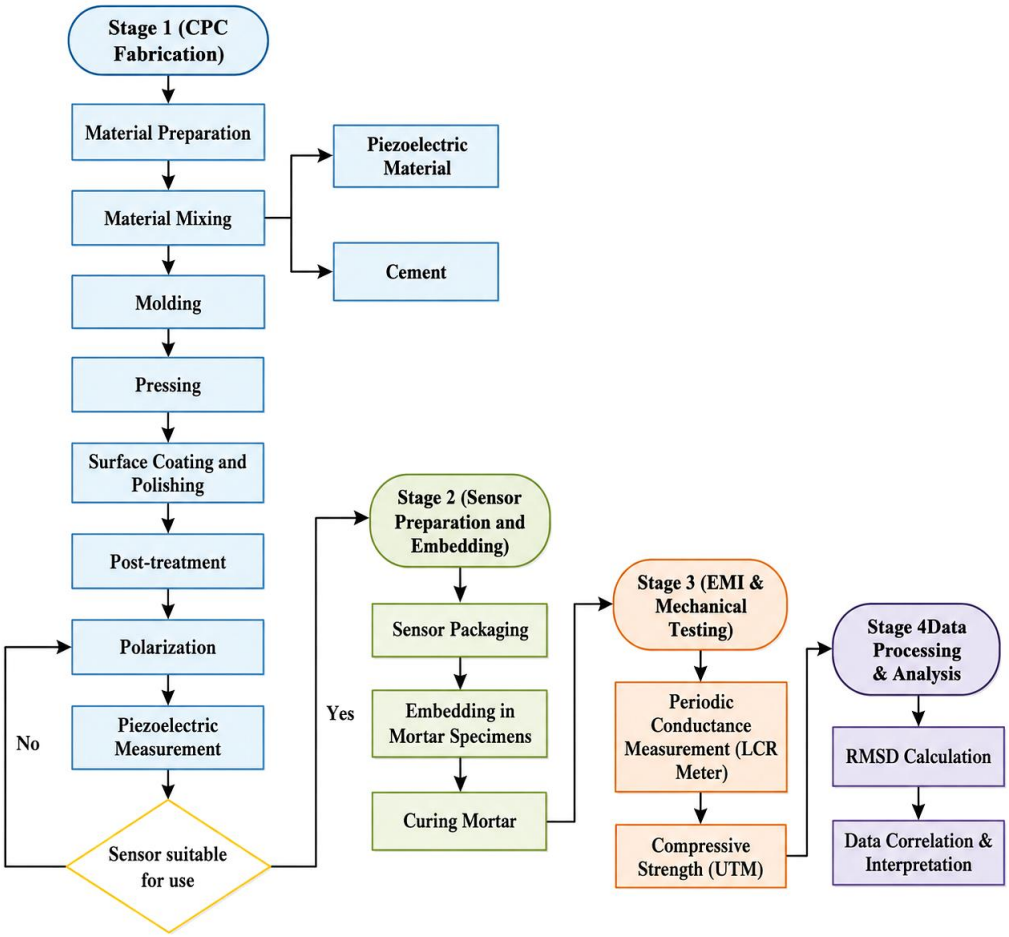

Figure 6. Schematic diagram illustrating the overall methodology used in this study

3. Results and Discussion

3.1. EMI Signatures as Indicators of Mechanical Property Evolution

The EMI response reflects the interaction between the CPC sensor and the surrounding mortar. As the hydration process progresses, the microstructure of the mortar becomes denser and stiffer, which in turn affects the vibration characteristics of the sensor. Within the effective frequency range, an increase in mortar stiffness is typically indicated by a decrease in conductance amplitude and a shift in the shape of the conductance curve. These variations indicate that the mechanical bond between the sensor and the mortar strengthens with age, allowing for the sensitive recording of mechanical changes in the mortar through the EMI signal.

The RMSD value of conductance is used to quantify the magnitude of the EMI signal difference from the baseline value. The higher the RMSD value, the greater the change in conductance, reflecting an increase in the stiffness and strength of the mortar. Thus, EMI signals, particularly conductance and conductance RMSD, are sensitive parameters for monitoring the evolution of mechanical properties and internal structural changes in mortar. This theoretical basis is fundamental to interpreting the experimental results presented.

3.2. Conductance and the Age

The conductance of mortar with embedded CPC sensors was measured on days 0, 7, 28, 56, and 90. Day 0 was chosen as the baseline for calculating the conductance deviation, which is the difference between the conductance value on a specific day and the conductance value on day 0. Day 0 is 6 hours after casting, which leads to the mortar setting time process. The conductance value is the average of 3 specimens on each test day. There are 48 specimens, each with a total of 4 variations. For comparison, a PZT patch sensor was embedded in the mortar, and its conductance was measured on the same day as the mortar using the CPC sensor. There were 12 mortar test specimens with embedded PZT patch sensors.

Figure 7 shows the conductance and frequency relationship curves for the four CPC variations. The four variations show a behavior where the conductance value increases with increasing frequency and decreases with increasing mortar age. This tendency implies that the electrical conductivity of mortar, as recorded by the CPCs, decreases with age. Several things can cause this phenomenon: 1) Hydration and microstructural changes. Over time, the mortar undergoes

a curing process, and the hydration process occurs, resulting in a denser microstructure. This reduces the porosity in it. In other words, the denser and more compact it is, the more difficult it becomes for electric charges to move through it. 2) Formation of an insulating phase. Over time, a less conductive phase or compound, such as C-S-H, is formed in the mortar. This phase surrounds the conductive particles in the composite, thereby inhibiting the ability to conduct electricity and reducing the overall conductance. 3) Reduction of ionic mobility. The more mortar is used, the less moisture content, even though this moisture content plays a role in ion transport. The reduced moisture content causes lower conductance. 4) Interface effect. Over time, the bonds at this interface can become more robust, inhibiting the free movement of charge carriers and thereby reducing conductance.

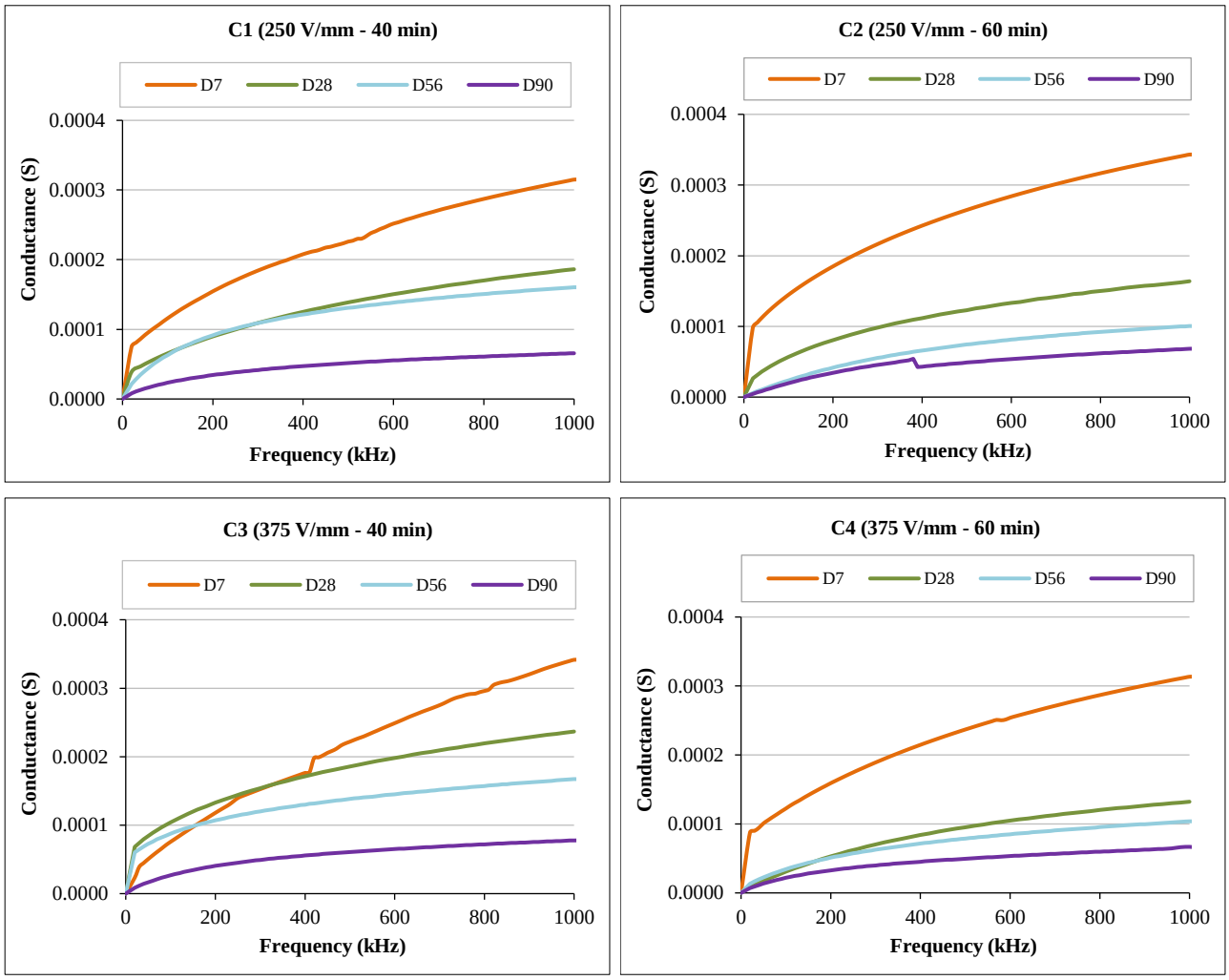

Figure 7. Conductance-frequency curves of CPC measured within the 20-1000 kHz frequency range

In Figure 7, there are also no frequency peaks, so it is easy to determine the effective frequency range. The effective frequency range is the range where the consistency conductance decreases with the increasing age of the mortar. This range is significant as it indicates the frequencies at which the mortar's conductance is most sensitive to changes in its age. Although they share a similar tendency, it can be observed that the effective frequency ranges of the four variations differ. C4 has the broadest frequency range, spanning 300-1000 kHz, followed by C2, C3, and C1, which range from 390-1000 kHz, 420-1000 kHz, and 500-1000 kHz, respectively. Sensors with a broader effective frequency range exhibit mechanical properties and electrical impedance more similar to those of mortar.

Figure 8 illustrates the conductance and frequency curves of the mortar specimens with embedded PZT patches. Unlike the conductance recorded by CPC, the conductance measured by PZT patches exhibits peaks at specific frequencies. Analysis of the conductance patterns recorded by PZT is quite challenging, due to the degree of randomness displayed. In specific frequency ranges, namely 325-435 kHz and 580-710 kHz, the conductance decreases with the mortar's age. This range is considered the effective frequency range. Notably, this frequency range is narrower than observed in the four preceding CPC variations. This suggests that the mechanical properties and acoustic impedance between the PZT patch sensor and the mortar do not surpass those of the CPC sensor.

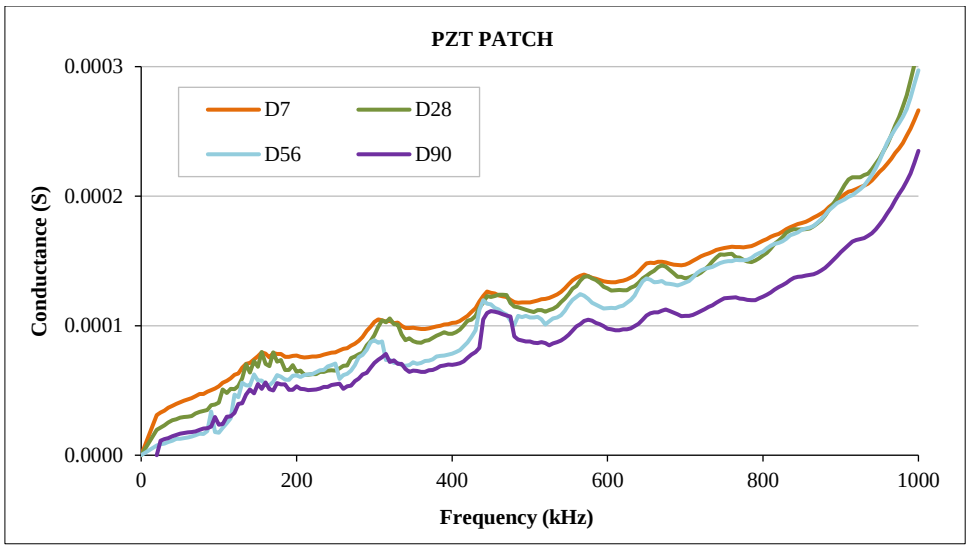

Figure 8. Conductance-frequency curves of the embedded PZT Patch used for comparison with CPC

Additionally, the conductance and frequency curves associated with the PZT patch are more complex than those of the CPC sensor. As a result, the CPC sensor demonstrates greater sensitivity to changes in conductance when fluctuations occur in the mortar conductance. Consequently, the CPC sensor is deemed more suitable for structural health monitoring (SHM) in cementitious materials. Table 1 compares the effective monitoring frequency ranges for all variants.

Table 1. Comparison of the effective frequency ranges of CPC and PZT sensors

Sensor Type	Effective Frequency Range (kHz)
C1	500-1000
C2	390-1000
C3	420-1000
C4	300-1000
PZT	325-435 and 580-710

3.3. Conductance and the Compressive Strength

Figure 9 presents a significant curve of the compressive strength and conductance corresponding to the ages of C4. This pattern was consistent across other variants like C1, C2, and C3, where the compressive strength increased, and the frequency decreased as the mortar age increased. The 450 kHz, 670 kHz, and 920 kHz were chosen to represent the effective monitoring frequency range, demonstrating that all frequencies within this range exhibited the same behavior. This finding highlights the potential of conductance within the effective monitoring frequency range for monitoring mortar strength when CPC is embedded inside the mortar. Table 2 further compares conductance at specific frequencies within the effective monitoring frequency range, highlighting the implications of these results for the field of materials science and engineering.

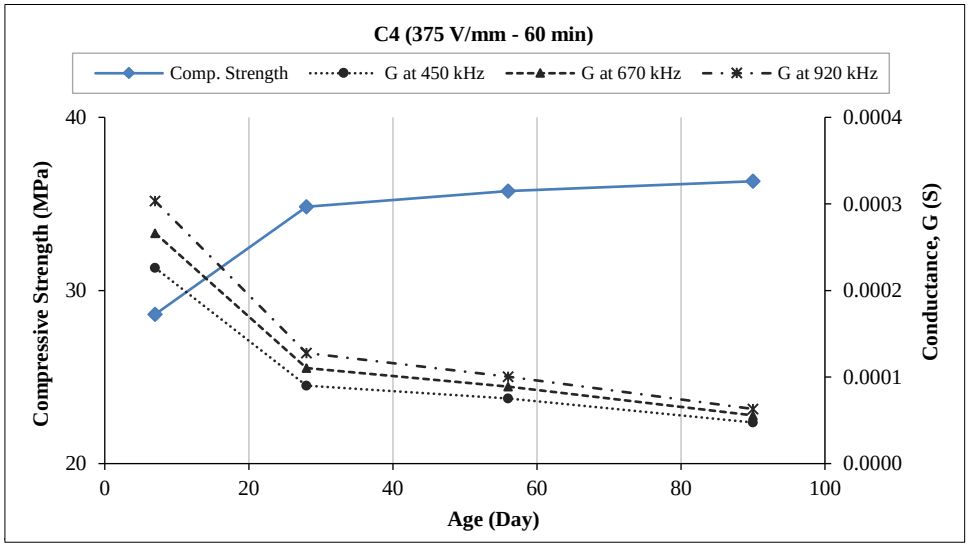

Figure 9. Comparison of C4 conductance at selected frequencies across different ages

Table 2. Comparison of CPC conductance values at selected frequencies across different ages

Sensor Type	Day	Conductance ($\times 10^{-4}$ S) at selected frequencies		
		450 kHz	670 kHz	920 kHz
C1	7	2,173	2,656	3,044
	28	1,321	1,578	1,802
	56	1,263	1,508	1,651
	90	0,495	0,575	0,638
C2	7	2,540	2,963	3,331
	28	1,177	1,396	1,582
	56	0,702	0,854	0,974
	90	0,658	0,568	0,658
C3	7	2,056	2,678	3,251
	28	1,788	2,061	2,301
	56	0,911	1,052	1,173
	90	0,564	0,657	0,737
C4	7	2,261	2,662	3,033
	28	0,899	1,105	1,278
	56	0,753	0,888	1,006
	90	0,475	0,557	0,631

The appearance of damage resulting from compression testing on 90-day-old mortar specimens containing embedded CPC is shown in Figure 10. The fact that damage mainly occurred on the outer surface of the cube, while the area around the CPC sensor remained intact without showing any cracks or debonding, is a significant observation. This indicates that the presence of CPC sensors did not cause the formation of weak areas or reduce the integrity of the mortar matrix. Small cracks on the surface were primarily observed in C1 and C3, while C2 and C4 exhibited a denser crack pattern, albeit limited to the surface, consistent with the higher stiffness and compressive strength of these two variations. These visual observations reinforce the finding that the embedded CPC sensor exhibits good compatibility with the surrounding mortar matrix, a crucial aspect for its application in structural health monitoring.

These visual observations further confirm that the presence of CPC sensors does not harm the structural integrity or compressive behavior of the mortar. On the contrary, CPC sensors remain mechanically stable and strongly bonded to the matrix even after 90 days of curing and compressive loading, demonstrating their effectiveness for long-term structural health monitoring applications in cement-based materials.

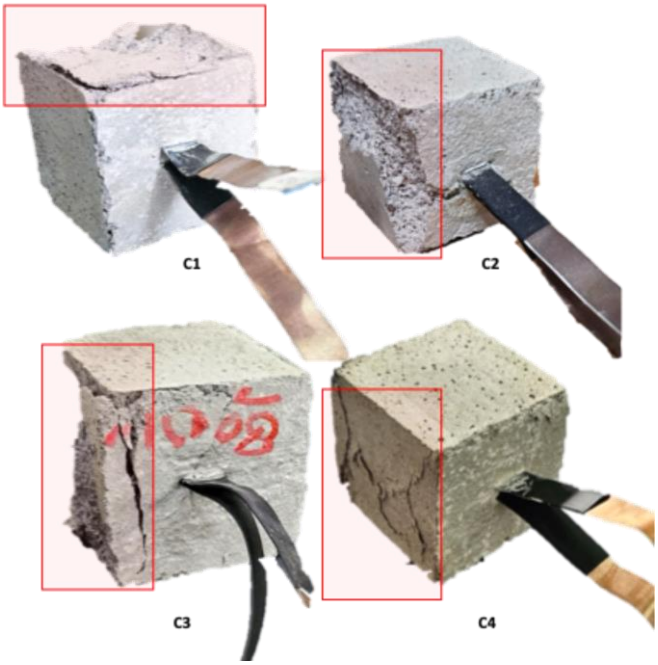

Figure 10. Compressive failure appearance of 90-day mortar specimens containing embedded CPC sensors (C1-C4)

3.4. RMSD of the Conductance and Compressive Strength

In monitoring compressive strength development over 90 days, the conductance value used was the conductance RMSD. This calculation was performed within the frequency range of each variation presented in Table 1. Figure 11 illustrates the relationship between compressive strength and RMSD of conductance, where both increase with mortar age. All four variations showed a significant increase in compressive strength, which occurred on day 28. The increase in compressive strength on days 56 and 90 was not significant. The highest compressive strength was demonstrated by C2, C4, C3, and C1 for the entire test day.

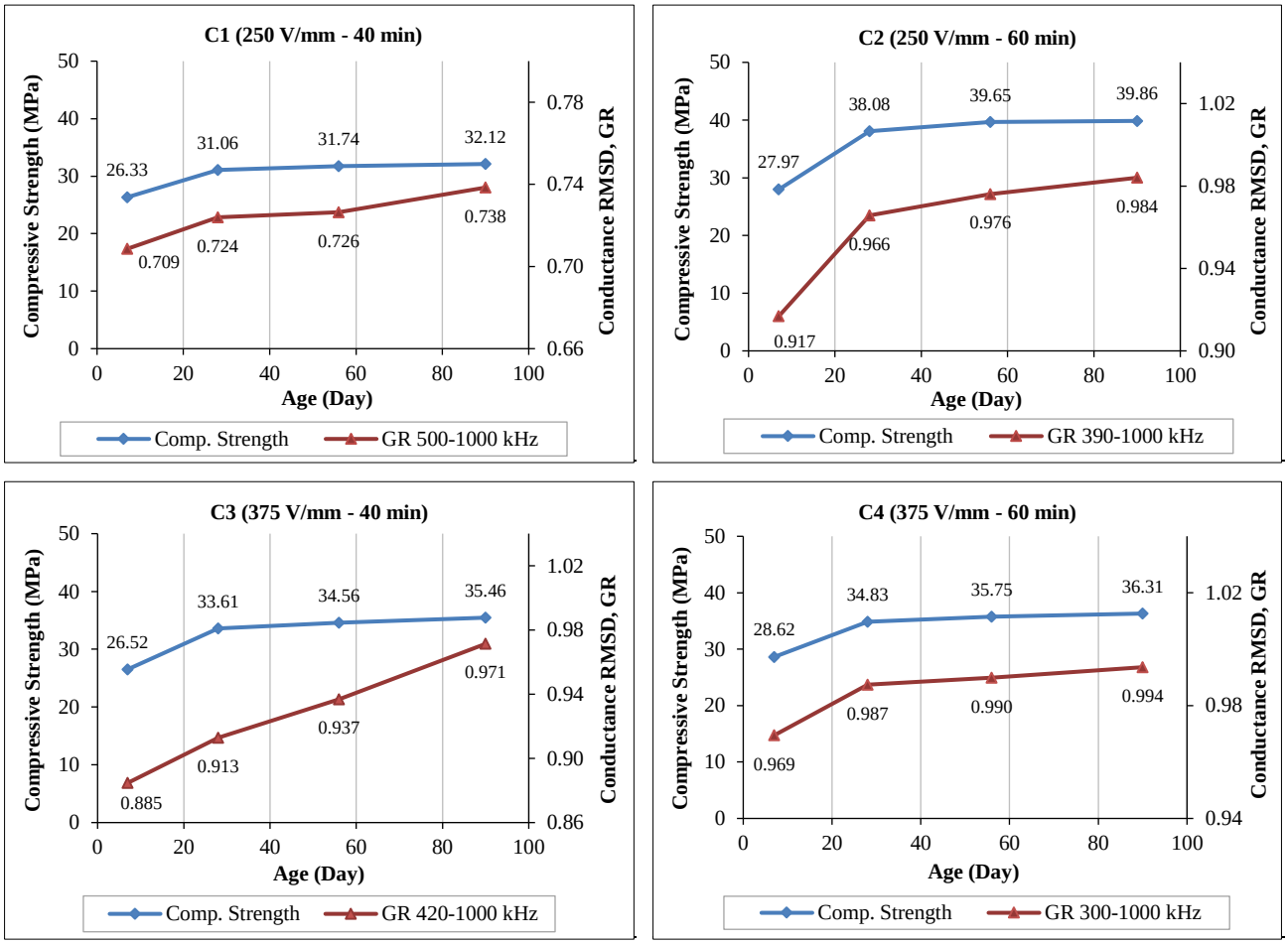

Figure 11. Comparison of compressive strength and conductance RMSD of CPC sensors over the 7, 28, 56, and 90 days

Regarding conductance RMSD, variations C2 and C4 increased in line with the compressive strength pattern, and the most significant change occurred on day 28. The increase in compressive strength of variation C2 on days 28, 56, and 90 was 36.1%, 4.1%, and 0.5%, respectively. While the increase in conductance RMSD of C2 variation on days 28, 56, and 90 was 5.3%, 1.1%, and 0.8% respectively. Next, the increase in compressive strength of variation C4 on days 28, 56, and 90 was 21.7%, 2.6%, and 1.6%. Meanwhile, the increase in conductance RMSD of variation C4 on days 28, 56, and 90 was 1.8%, 0.2%, and 0.4%, respectively. The increase in compressive strength of variation C1 on days 28, 56, and 90 was 17.9%, 2.2%, and 1.2%, respectively. Meanwhile, the increase in conductance RMSD of variation C1 on days 28, 56, and 90 was 2.2%, 0.3%, and 1.7%. Next, the increase in compressive strength of variation C3 on days 28, 56, and 90 was 26.7%, 2.8%, and 2.6%. Meanwhile, the increase in conductance RMSD of variation C3 on days 28, 56, and 90 was 3.2%, 2.6%, and 3.7%. The higher conductance values of C1 and C3, depicted in Figure 7, do not guarantee a good response from the CPC sensor to the development of compressive strength. This is indicated by an increase in the RMSD conductance percentage that is not synchronized with the increase in the compressive strength percentage. The RMSD conductance values, a significant indicator of sensor C1 and C3, are lower than those of C2 and C4, indicating a lower level of sensitivity.

Figure 11 shows the compressive strength and conductance RMSD curve for the four CPC variations. Sensors C3, C2, C1, and C4 have the lowest to highest baseline conductance. The conductance value drops as the mortar ages due to its increasing density and strength, making it more resistive. C4 shows the most significant decrease in conductance value, followed by C2, C1, and C3. Thus, C4 has the most considerable RMSD conductance value, with a range of

0.969-0.994. C2 has a conductance RMSD of 0.917-0.984, followed by C3 and C1 with ranges of 0.885-0.971 and 0.709-0.738, respectively. As a mortar ages, its density increases, thereby improving its insulating properties. This improvement in insulating properties causes the conductance signal recorded in the mortar to become weaker. A higher RMSD indicates a more significant difference between the baseline conductance (6 hours after casting) and the conductance on the reference days (days 7, 28, 56, and 90). Sensors with higher RMSD indicate higher sensitivity in responding to microstructural changes (possibly due to stress, strain, or damage) in the mortar detected through the weakening of the conductance signal.

Referring to Figure 7, the conductance values of C1 and C3 are indeed higher than those of C2 and C4. However, the changes in conductance RMSD values of C1 and C3 are not as good or synchronous as those of C2 and C4 regarding the development of their compressive strength. This means that the conductance recorded at baseline and on the reference days is not significantly different, so it does not sufficiently represent the microstructural changes that occur as the mortar hydrates. Although C1 and C3 show higher absolute conductance values, their RMSD correlation is poorer. This behavior can be associated with the interface effect and local moisture retention around the sensor. Moisture trapped at the electrode–matrix or PZT–matrix interface can maintain the ionic conductive pathways even as the mortar becomes denser with aging. This condition results in high conductivity but reduced sensitivity to age-related microstructural evolution. In addition, imperfect interfacial bonding may introduce alternative conduction routes that distort the relationship between conductance evolution and hydration-driven densification. Consequently, the conductance values of C1 and C3 do not change significantly between the baseline and reference ages, resulting in a lower RMSD correlation despite higher absolute conductance. A similar environmental effect was discussed by Ye et al. [44], who reported that variations in temperature and humidity significantly influence EMI signals due to changes in local dielectric and conductive properties

The results of conductance, RMSD, and compressive strength, as depicted in Figure 12, in this study are consistent with those of previous studies [25, 27, 32]. Previous studies have shown that conductance is a key parameter in EMI techniques for monitoring the development of mortar and concrete compressive strength. Su et al. [43] employed the PZT sensor-EMI technique to monitor the development of mortar strength at very early ages (4–8 hours) to early ages (1–7 days), with a frequency range of 100–400 kHz, compared to the baseline at 4 hours. The conductance spectrum shifted toward higher frequencies, indicating an increase in stiffness due to the hydration process, and the RMSD index of conductance showed a very high linear correlation with compressive strength. Pan & Huang [25, 27] extended this concept to concrete and mortar by comparing pure PZT sensors and CPC sensors that had been polarized at 1.5 kV/mm for 40 minutes at a temperature of 150 °C. The results showed that the real part of the conductance provided a better correlation with compressive strength than the susceptance. Furthermore, CPC exhibits a much wider effective frequency range than pure PZT (e.g., 300–660 kHz in Pan & Huang, 2019, and even 800–2000 kHz in Pan & Huang, 2020), and its conductance curve is smoother, without showing sharp resonances. This facilitates the selection of stable and representative monitoring frequencies. Furthermore, Pan & Guan [32] showed that CPCs polarized under the same conditions can detect voltage increases in concrete, where conductance decreases as voltage increases. The effective frequency range of CPC (815–1000 kHz) is also more stable than that of pure PZT, which has a much narrower range (20–35 kHz) and is more fluctuating.

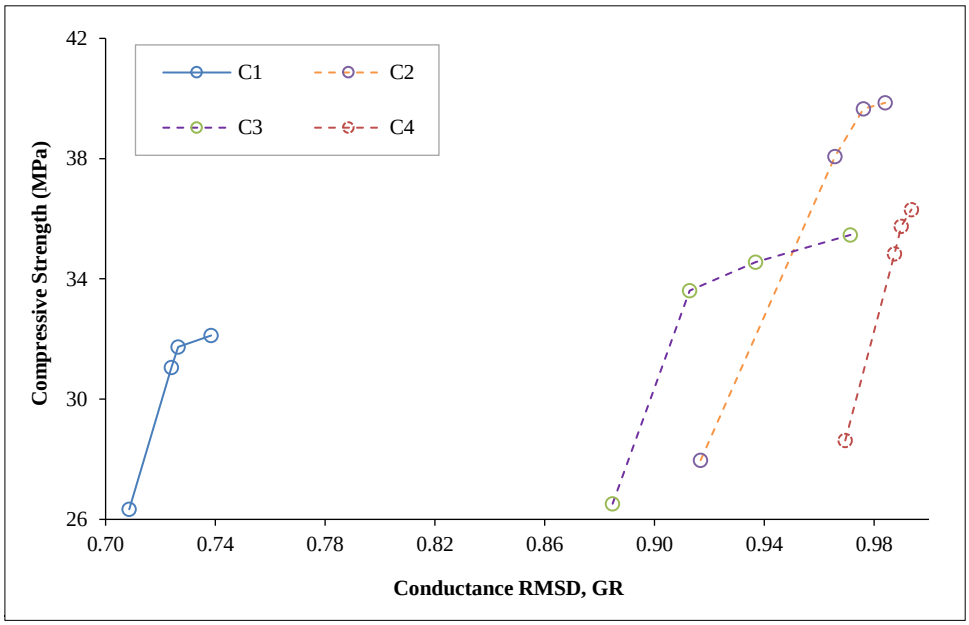

Figure 12. Conductance RMSD versus compressive strength curves for all CPC variations

Overall, these studies confirm that changes in conductance are a sensitive indicator of the evolution of the mechanical properties of cement-based materials, and RMSD of conductance is an effective quantitative index for linking changes in the EMI spectrum with strength development. Furthermore, cement-based sensors such as CPC have intrinsic advantages over pure PZT, namely matrix compatibility and a wider effective frequency range, which implies better signal sensitivity and stability for in-situ compressive strength monitoring applications. As mentioned by Pereira et al. [36], signals obtained through the EMI technique are "intrinsically linked to structural conditions" and therefore have the potential not only for damage detection but also for continuous performance monitoring of structural systems. By mapping changes in these impedance signals, this technique can evolve from a simple damage indicator to a comprehensive condition monitoring tool.

3.5. The Potential Use of CPCs

This study employed low electric fields of 250 V/mm and 375 V/mm, with durations of 40 and 60 minutes. The external electric field plays an important role in the polarization process. The polarization process aims to align the electric dipoles in the piezoelectric material in a uniform orientation. Aligning the electric dipoles induces microstructural changes that affect both mechanical and electrical properties. The electric field serves as a driving force for aligning piezoelectric domains within the matrix. A low electric field means a low driving force, resulting in limited and gradual dipole alignment. The interaction between PZT particles and C-S-H still occurred, but it is not significant enough to reorient the structure. Therefore, the quality of domain alignment is not as good as that of the high electric field (as evident from the d_{33} value, which tends to be lower than that of the high electric field); however, the risk of microcrack and ITZ degradation is lower. Conversely, a high electric field provides a much stronger electrostatic force, allowing the PZT domains to align more quickly and intensely. However, this condition has the potential to produce large local stress concentrations, triggering debonding at the PZT and C–S–H interface and promoting the formation of microcracks due to overstress. Therefore, a high electric field can produce stronger polarization, but it risks disrupting microstructural stability. Meanwhile, a low electric field produces more limited polarization, but it is safer in maintaining the integrity of the CPC microstructure. The results of this study indicate that a low electric field has promising potential when applied to mortar to observe the development of compressive strength.

Among the four variations, C4 has the highest baseline conductance, indicating better initial electrical properties, such as low resistance and potentially higher sensitivity. Conductance RMSD reflects the variation of conductance during the test, which is affected by 1) changes in external stimuli (e.g., stress and damage) and 2) the sensor's response to load. Based on the conductance RMSD values, C4 and C2 have higher values than C1 and C3. This value indicates higher sensitivity and makes them more responsive to changes in the mortar's conductance. Regarding compressive strength, mortars with embedded sensors C2 and C4 showed higher compressive strength values than C1 and C3 for all days of testing. Polarization with a longer duration of 60 minutes resulted in better dipole alignment. This better dipole alignment improves the CPC's structural integrity and mechanical properties, making it less susceptible to cracking or stress concentration under load. The Interfacial Transition Zone (ITZ) is a critical area where the sensor property and the surrounding mortar interact. A more substantial and consistent ITZ can transfer stresses well between the CPC sensor and the mortar. C2 and C4, sensors with better piezoelectric properties due to prolonged polarization, can interact more effectively with the hydrated cement paste, resulting in a denser and more homogeneous ITZ. C1 and C3, with shorter polarization duration sensors, result in weaker piezoelectric properties and less favorable ITZ microstructure, reducing the overall compressive strength. More prolonged polarization may also affect the surface characteristics of the CPC sensor, which can improve its bonding with the mortar, leading to better stress distribution during the pressing process. This is confirmed by the test results, which show that crushing during pressing does not occur at the interface of CPC and mortar.

The interfacial conditions between the CPC sensor and mortar are the main factors that influence the stability of EMI responses. Localized moisture retention, weak bonding, and the presence of unhydrated layers can alter local dielectric properties and electrical pathways, thereby affecting EMI signals. The effects of micro-scale environments on EMI are comparable to those of macro-scale influences, as reported in the literature, where temperature and humidity fluctuations significantly affect impedance signatures. Consequently, the quality of the CPC-mortar interface must be strong to ensure accurate and repeatable EMI sensing.

All four CPC variations demonstrated their ability to detect conductance degradation for up to 90 days. C4 and C2 are better choices when high sensitivity and superior mechanical strength are critical to the application. The sensitivity makes them detect small changes effectively, and their high compressive strength ensures good durability. However, C1 and C3 sensors still have relatively high RMSD values. The conductance and conductance RMSD values indicate that C1 and C3 are preferable if long-term stability of electrical properties is the primary concern, as they demonstrate better consistency in conductance over time.

Previous EMI research predominantly focuses on damage detection; identifying cracks, stiffness loss, or material degradation. However, the same electromechanical principles can be applied to monitor the development of strength in cementitious materials by observing the evolution of early-age and long-term stiffness. The CPC–EMI method amplifies the range of EMI, not only detecting damage but also witnessing the growth of the material's strength. This is the case as the basic and practical aspects of EMI-based structural monitoring are enlarged.

4. Conclusions

Several key conclusions can be drawn from the findings of this study:

- First, the effective frequency range of CPC is wider than that of PZT sensors. In this study, C4 exhibited the widest effective bandwidth. The significance of this wider bandwidth is not merely the extent of the frequency range; rather, it indicates that CPC (especially C4) provides a broader frequency interval in which changes in conductance due to mechanical variations in mortar can be recorded reliably. In other words, a wider effective frequency range allows greater flexibility in selecting reliable monitoring frequencies in EMI techniques.
- Second, within the effective frequency range, all sensors showed a consistent conductance trend: conductance increased with increasing frequency but decreased with increasing mortar age. This trend aligns with the hydration and densification processes of mortar, which make the material stiffer and more insulating, resulting in a lower recorded conductance signal at later ages.
- Third, conductance, RMSD, and compressive strength increased over time across all sensor types. Among the variations, C2 and C4 demonstrated a more synchronized correlation between increasing conductance RMSD and compressive strength, suggesting more reliable sensing performance. Notably, C4 recorded the highest RMSD conductance values, indicating superior sensitivity in detecting changes within the mortar. This sensitivity, combined with strong mechanical performance, makes C4 the most effective sensor when high sensitivity and mechanical strength are required.
- Fourth, high conductance values do not always correspond to high RMSD values, as observed in C1 and C3. These sensors had the shortest polarization duration in this study, resulting in lower poling efficiency. Suboptimal poling may lead to a less compact PZT–matrix interface and local moisture retention in the ITZ zone. These conditions can sustain ionic conductive pathways, producing high absolute conductance values; however, the signal changes become less sensitive to matrix densification as the mortar ages. Consequently, the resulting RMSD values are lower and do not accurately reflect the actual microstructural changes occurring in the material.
- Finally, the results confirm that cement-based piezoelectric composites (CPCs), polarized under a low electric field, are capable of monitoring the development of compressive strength and changes in conductance in mortar for up to 90 days. This highlights their potential for long-term structural health monitoring applications.

5. Declarations

5.1. Author Contributions

Conceptualization, G.A.H. and W.S.; methodology, W.S.; validation, G.A.H. and K.D.W.; formal analysis, G.A.H. and W.S.; investigation, G.A.H. and K.D.W.; data curation, W.S.; writing—original draft preparation, G.A.H.; writing—review and editing, W.S. and P.S.; visualization, G.A.H.; supervision, W.S. and P.S.; funding acquisition, P.S. and W.S. All authors have read and agreed to the published version of the manuscript.

5.2. Data Availability Statement

The data presented in this study are available in the article.

5.3. Funding and Acknowledgments

The authors would also like to acknowledge the vote of thanks to the Indonesian Endowment Fund for Education / Lembaga Pengelola Dana Pendidikan (LPDP) from the Ministry of Finance; Ministry of Research, Technology and Higher Education Indonesia; and Sepuluh Nopember Institute of Technology (ITS) for the financial support.

5.4. Conflicts of Interest

The authors declare no conflict of interest.

6. References

[1] Santos, J. A., Sanches, A. O., Akasaki, J. L., Tashima, M. M., Longo, E., & Malmonge, J. A. (2020). Influence of PZT insertion on Portland cement curing process and piezoelectric properties of 0–3 cement-based composites by impedance spectroscopy. Construction and Building Materials, 238. doi:10.1016/j.conbuildmat.2019.117675.

[2] Ma, Y., Jiang, Q., Dai, J., & Li, Y. (2022). Influence of PZT volume fraction, composite thickness and cement matrix on the performance of d15 shear mode 1–3 connectivity cement-based piezoelectric composites. Construction and Building Materials, 329. doi:10.1016/j.conbuildmat.2022.127190.

[3] Qin, L., Lu, Y., & Li, Z. (2010). Embedded Cement-Based Piezoelectric Sensors for Acoustic Emission Detection in Concrete. Journal of Materials in Civil Engineering, 22(12), 1323–1327. doi:10.1061/(asce)mt.1943-5533.0000133.

[4] Rathod, V. T. (2020). A Review of Acoustic Impedance Matching Techniques for Piezoelectric Sensors and Transducers. Sensors, 20(14), 4051. doi:10.3390/s20144051.

[5] Shifeng, H., Zhengmao, Y., Dongyu, X., Jun, C., Shoude, W., & Xin, C. (2007). Fabrication and properties of 2-2 cement based piezoelectric composites. Ferroelectrics, Letters Section, 34(1–2), 22–28. doi:10.1080/07315170701313690.

[6] Hayu, G. A., Sutrisno, W., Wulandari, K. D., Suprobo, P., & Irawan, M. (2024). Development of Cement-Based Piezoelectric Ceramic Composite as an Innovative Sensing Element and the Potential Use of Industrial Waste: a Review. International Review of Civil Engineering, 15(4), 311–324. doi:10.15866/irece.v15i4.24083.

[7] Ding, W., Liu, Y., Shiotani, T., Wang, Q., Han, N., & Xing, F. (2021). Cement-based piezoelectric ceramic composites for sensing elements: A comprehensive state-of-the-art review. Sensors, 21(9), 3230. doi:10.3390/s21093230.

[8] Gong, H., Zhang, Y., Quan, J., & Che, S. (2011). Preparation and properties of cement based piezoelectric composites modified by CNTs. Current Applied Physics, 11(3), 653–656. doi:10.1016/j.cap.2010.10.021.

[9] Zhao, P., Wang, S., Kadlec, A., Li, Z., & Wang, X. (2016). Properties of cement–sand-based piezoelectric composites with carbon nanotubes modification. Ceramics International, 42(13), 15030–15034. doi:10.1016/j.ceramint.2016.06.153.

[10] Chaipanich, A., Rianyoi, R., Potong, R., & Jaitanong, N. (2014). Aging of 0–3 piezoelectric PZT ceramic–Portland cement composites. Ceramics International, 40(8), 13579–13584. doi:10.1016/j.ceramint.2014.05.073.

[11] Zhang, F., Feng, P., Wang, T., & Chen, J. (2019). Mechanical-electric response characteristics of 1-3 cement based piezoelectric composite under impact loading. Construction and Building Materials, 228. doi:10.1016/j.conbuildmat.2019.116781.

[12] Sappati, K. K., & Bhadra, S. (2018). Piezoelectric Polymer and Paper Substrates: A Review. Sensors, 18(11), 3605. doi:10.3390/s18113605.

[13] Hunpratub, S., Yamwong, T., Srilomsak, S., Maensiri, S., & Chindaprasirt, P. (2014). Effect of particle size on the dielectric and piezoelectric properties of 0–3BCTZO/cement composites. Ceramics International, 40(1), 1209–1213. doi:10.1016/j.ceramint.2013.05.118.

[14] Wittinanon, T., Rianyoi, R., Ngamjarurojana, A., & Chaipanich, A. (2020). Effect of polyvinylidene fluoride on the acoustic impedance matching, poling enhancement and piezoelectric properties of 0–3 smart lead-free piezoelectric Portland cement composites. Journal of Electroceramics, 44(3–4), 232–241. doi:10.1007/s10832-020-00214-7.

[15] Lee, H. J., Zhang, S., Bar-Cohen, Y., & Sherrit, S. (2014). High temperature, high power piezoelectric composite transducers. Sensors (Switzerland), 14(8), 14526–14552. doi:10.3390/s140814526.

[16] Li, Z., Zhang, D., & Wu, K. (2002). Cement-based 0-3 piezoelectric composites. Journal of the American Ceramic Society, 85(2), 305-313. doi:10.1111/j.1151-2916.2002.tb00089.x.

[17] Wang, F., Wang, H., Song, Y., & Sun, H. (2012). High piezoelectricity 0-3 cement-based piezoelectric composites. Materials Letters, 76, 208–210. doi:10.1016/j.matlet.2012.02.094.

[18] Potong, R., Rianyoi, R., Ngamjarurojana, A., Yimnirun, R., Guo, R., Bhalla, A. S., & Chaipanich, A. (2013). Effect of particle size on dielectric properties and hysteresis behavior of 0-3 barium zirconate titanate-portland cement composites. Integrated Ferroelectrics, 148(1), 131–137. doi:10.1080/10584587.2013.852057.

[19] Chomyen, P., Potong, R., Rianyoi, R., Ngamjarurojana, A., Chindaprasirt, P., & Chaipanich, A. (2018). Microstructure, dielectric and piezoelectric properties of 0–3 lead free barium zirconate titanate ceramic-Portland fly ash cement composites. Ceramics International, 44(1), 76–82. doi:10.1016/j.ceramint.2017.09.112.

[20] Yang, Y., Li, P., Lin, M., Li, X., Li, S., Chai, Y., & Li, L. (2025). A Comprehensive Review of Cement-Based Piezoelectric Composites: Configurations, Performance and Application. Journal of Electronic Materials, 54(10), 8239–8258. doi:10.1007/s11664-025-12244-4.

[21] Ma, Y., Yao, C., Zhang, X., Jiang, Q., & Zhou, C. (2024). Mechanical-electric response characteristics of 1–3 connectivity pattern cement-based piezoelectric composite sensors with varying functional phase parameters under impact loading. Construction and Building Materials, 453, 139101. doi:10.1016/j.conbuildmat.2024.139101.

[22] Parvanova, V. D., & Nadoliisky, M. M. (2005). Polarization processes in PZT ceramics. Bulgarian Journal of Physics, 32, 45-50.

[23] Li, Z., Dong, B., & Zhang, D. (2005). Influence of polarization on properties of 0-3 cement-based PZT composites. Cement and Concrete Composites, 27(1), 27–32. doi:10.1016/j.cemconcomp.2004.02.001.

[24] Ding, W., Xu, W., Dong, Z., Liu, Y., Wang, Q., & Shiotani, T. (2021). Influence of hydration capacity for cement matrix on the piezoelectric properties and microstructure of cement-based piezoelectric ceramic composites. Materials Characterization, 179, 111390. doi:10.1016/j.matchar.2021.111390.

[25] Pan, H. H., & Huang, M. W. (2020). Piezoelectric cement sensor-based electromechanical impedance technique for the strength monitoring of cement mortar. Construction and Building Materials, 254, 119307. doi:10.1016/j.conbuildmat.2020.119307.

[26] Pan, H. H., Wang, C. K., & Cheng, Y. C. (2016). Curing time and heating conditions for piezoelectric properties of cement-based composites containing PZT. Construction and Building Materials, 129, 140–147. doi:10.1016/j.conbuildmat.2016.10.107.

[27] Pan, H.-H., Wong, Y.-D., & Su, Y.-M. (2019). Piezoelectric cement sensor and impedance analysis for concrete health monitoring. SPIE Proceedings, 33, 2514306. doi:10.1117/12.2514306.

[28] Jaitanong, N., & Chaipanich, A. (2008). Effect of poling temperature on piezoelectric properties of 0-3 PZT-Portland cement composites. Ferroelectrics, Letters Section, 35(1–2), 17–23. doi:10.1080/07315170801992179.

[29] Chaipanich, A. (2007). Dielectric and piezoelectric properties of PZT-silica fume cement composites. Current Applied Physics, 7(5), 532–536. doi:10.1016/j.cap.2006.10.016.

[30] Li, H., Di, B., Zheng, Y., Ma, H., Huang, X., Wu, H., & Zhang, J. (2025). Concrete Damage Identification and Localization for Structural Health Monitoring Based on Piezoelectric Sensors. Sensors, 25(8), 2532. doi:10.3390/s25082532.

[31] Jothi Saravanan, T., Balamonica, K., Bharathi Priya, C., Gopalakrishnan, N., & Murthy, S. G. N. (2017). Piezoelectric EMI–Based Monitoring of Early Strength Gain in Concrete and Damage Detection in Structural Components. Journal of Infrastructure Systems, 23(4), 04017029. doi:10.1061/(asce)is.1943-555x.0000386.

[32] Pan, H. H., & Guan, J. C. (2022). Stress and strain behavior monitoring of concrete through electromechanical impedance using piezoelectric cement sensor and PZT sensor. Construction and Building Materials, 324, 126685. doi:10.1016/j.conbuildmat.2022.126685.

[33] Gedam, S. R., & Khante, S. N. (2016). Experimental Investigation on Sensitivity of Smart Aggregate Embedded in Reinforced Concrete Beam. Open Journal of Civil Engineering, 6(4), 653–669. doi:10.4236/ojce.2016.64053.

[34] Wang, T., Tan, B., Lu, M., Zhang, Z., & Lu, G. (2020). Piezoelectric electro-mechanical impedance (EMI) based structural crack monitoring. Applied Sciences (Switzerland), 10(13), 4648. doi:10.3390/app10134648.

[35] Zhu, H., Luo, H., Ai, D., & Wang, C. (2016). Mechanical impedance-based technique for steel structural corrosion damage detection. Measurement, 88, 353-359. doi:10.1016/j.measurement.2016.01.041.

[36] Pereira, P. E. C., de Rezende, S. W. F., Fernandes, H. C., de Moura Junior, J. dos R. V., & Finzi Neto, R. M. (2024). On damage location techniques and future prospects for industrial applications utilizing the electromechanical impedance method: a systematic review. Journal of the Brazilian Society of Mechanical Sciences and Engineering, 46(5), 4916. doi:10.1007/s40430-024-04916-9.

[37] Tressler, J. F., Alkoy, S., & Newnham, R. E. (1998). Piezoelectric sensors and sensor materials. Journal of Electroceramics, 2(4), 257-272. doi:10.1023/A:1009926623551.

[38] Tiantong, P., Bongkarn, T., Rianyoi, R., & Julphunthong, P. (2022). Fabrication and characterisation of 0-3 KNLNTS piezoelectric ceramic/alite calcium sulfoaluminate cement composites. Journal of Materials Research and Technology, 19, 1563–1577. doi:10.1016/j.jmrt.2022.05.136.

[39] Shifeng, H., Jun, C., Futian, L., Lingchao, L., Zhengmao, Y., & Xin, C. (2004). Poling process and piezoelectric properties of lead zirconate titanate/sulphoaluminate cement composites. Journal of materials science, 39(23), 6975-6979. doi:10.1023/B:JMSC.0000047540.71855.3a.

[40] Dong, B., & Li, Z. (2005). Cement-based piezoelectric ceramic smart composites. Composites Science and Technology, 65(9), 1363-1371. doi:10.1016/j.compscitech.2004.12.006.

[41] Hayu, G. A., Sutrisno, W., Wulandari, K. D., & Suprobo, P. (2024). Effect of Low Electric Field Polarization Condition on Properties of Cement-based Piezoelectric Ceramic Composite. Civil Engineering and Architecture, 12(6), 3759-3771. doi:10.13189/cea.2024.120603.

[42] Ding, W., Xu, W., Dong, P., Liu, Y., & Shiotani, T. (2022). Roles of CSH gel in the microstructure and piezoelectric properties variation of cement-based piezoelectric ceramic composite. Materials Letters, 306, 130952. doi:10.1016/j.matlet.2021.130952.

[43] Su, Y. F., Han, G., Amran, A., Nantung, T., & Lu, N. (2019). Instantaneous monitoring the early age properties of cementitious materials using PZT-based electromechanical impedance (EMI) technique. Construction and Building Materials, 225, 340–347. doi:10.1016/j.conbuildmat.2019.07.164.

[44] Ye, Y., Zhu, Y., Lei, B., Weng, Z., Xu, H., & Wan, H. (2024). An approach for structural damage identification using electromechanical impedance. Structural Monitoring and Maintenance, 11(3), 203–217. doi:10.12989/smm.2024.11.3.203.